

Identification of Selective, Nonpeptidic Nitrile Inhibitors of Cathepsin S Using the Substrate Activity Screening Method

Andrew W. Patterson,[†] Warren J. L. Wood,[†] Michael Hornsby,[‡] Scott Lesley,[‡] Glen Spraggon,^{*,‡} and Jonathan A. Ellman^{*,†}

Department of Chemistry, University of California, Berkeley, California 94720, and Genomics Institute of the Novartis Research Foundation, 10675 John Jay Hopkins Drive, San Diego, California 92121

Received June 10, 2006

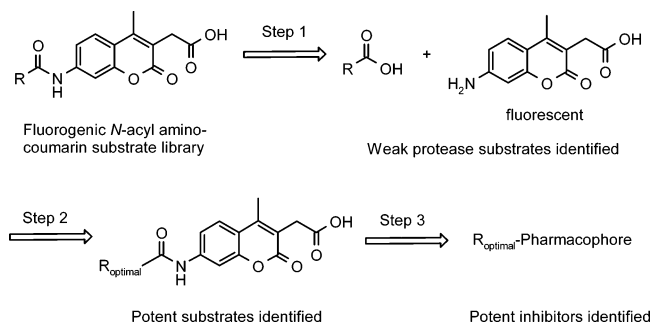
The substrate activity screening method, a substrate-based fragment identification and optimization method for the development of enzyme inhibitors, was previously applied to cathepsin S to obtain low nanomolar 1,4-disubstituted-1,2,3-triazole-based aldehyde inhibitors (Wood, W. J. L.; Patterson, A. W.; Tsuruoka, H.; Jain, R. K.; Ellman, J. A. *J. Am. Chem. Soc.* **2005**, *127*, 15521–15527). Replacement of the metabolically labile aldehyde pharmacophore with the nitrile pharmacophore provided inhibitors with moderate potency for cathepsin S. The inhibitors showed good selectivity over cathepsins B and L but no selectivity over cathepsin K. X-ray structures of two crystal forms (1.5 and 1.9 Å) of a complex between cathepsin S and a triazole inhibitor incorporating a chloromethyl ketone pharmacophore guided the design of triazole substrates with increased cleavage efficiency and selectivity for cathepsin S over cathepsins B, L, and K. Conversion of select substrates to nitrile inhibitors yielded a low molecular weight (414 Da) and potent (15 nM) cathepsin S inhibitor that showed >1000-fold selectivity over cathepsins B, L, and K.

Introduction

We recently disclosed the first substrate-based fragment identification and optimization approach for the development of novel, nonpeptidic protease inhibitors called substrate activity screening (SAS; Scheme 1).^{1,2,3} In the first step of the three-step process, a library of *N*-acyl aminocoumarins are screened to identify protease substrates using a high throughput, continuous fluorescence-based assay. False positives due to aggregation, protein precipitation, or nonspecific binding are not observed because active enzyme and productive active site binding are required for the protease-catalyzed amide bond hydrolysis that releases the fluorescent coumarin group.⁴ In step 2, the activity of the substrates is rapidly optimized by the synthesis and subsequent assay of focused libraries of substrate analogues. Step 3 then builds upon a key attribute of this mechanism-based substrate screen, namely, that the *N*-acyl aminocoumarin must be precisely oriented in the active site to enable productive substrate cleavage, and therefore, the aminocoumarin can be replaced with mechanism-based pharmacophores to directly provide protease inhibitors. The choice and versatility of pharmacophores allows reversible or irreversible inhibitors to be rapidly obtained once efficient substrates are identified.

We applied the SAS method to the cysteine protease cathepsin S, which is involved in the final step of the degradation of the invariant chain necessary for antigen presentation and subsequent immune response and is consequently implicated in autoimmune diseases such as rheumatoid arthritis and multiple sclerosis,⁵ as well as tumor development and growth.⁶ Multiple distinct classes of nonpeptidic substrates to cathepsin S were identified upon screening a *N*-acyl aminocoumarin library. Select substrates were optimized and then directly converted to highly novel, low molecular weight, nonpeptidic aldehyde inhibitors with nanomolar affinity to cathepsin S.¹

Scheme 1. Outline of the Substrate Activity Screening Method



The 1,4-disubstituted-1,2,3-triazole-based aldehyde inhibitors **1** and **2** (Figure 1) were the most potent compounds to be identified toward cathepsin S using the SAS method and represent promising inhibitor structures as a result of their novelty and nonpeptidic character. However, in our initial publication, we did not address whether selective triazole-based inhibitors could be obtained. Moreover, the aldehyde pharmacophore is not desirable because it is a very reactive electrophile that may lack selectivity *in vivo* and is rapidly metabolized. Here we report on the development of triazole-based inhibitors with greater than 1000-fold selectivity for cathepsin S over the highly homologous papain family human cathepsins B, K, and L⁷ and that incorporate the more desirable, clinically validated nitrile⁸ rather than the aldehyde pharmacophore.

Chemistry

The synthesis of 1,4-disubstituted-1,2,3-triazole substrates and inhibitors required the preparation of enantiomerically pure chiral propargylamine intermediates, which was accomplished by a 1,2-addition of lithiated (trimethylsilyl)acetylene to *N*-*tert*-butanesulfinyl ketimines **3** (Scheme 2).^{9,10} The additions proceeded with uniformly high diastereoselectivities (97:3 to >99:1 d.r.) to generate the sulfinamide intermediates **4**. Chromatography provided diastereomerically pure material, which after silyl and sulfinyl group removal gave the enantiomerically pure propargylamine salts **6**.

* Corresponding authors. E-mail: jellman@uclink.berkeley.edu (J.A.E.); gspraggon@gnf.org (G.S.). Tel.: 510-642-4488 (J.A.E.); 858-812-1567 (G.S.). Fax: 510-642-8369 (J.A.E.); 858-812-1746 (G.S.).

[†] The University of California-Berkeley.

[‡] Genomics Institute of the Novartis Research Foundation.

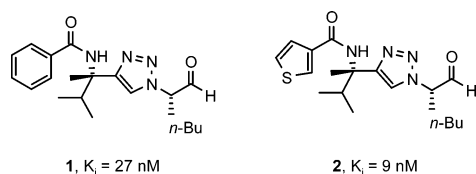
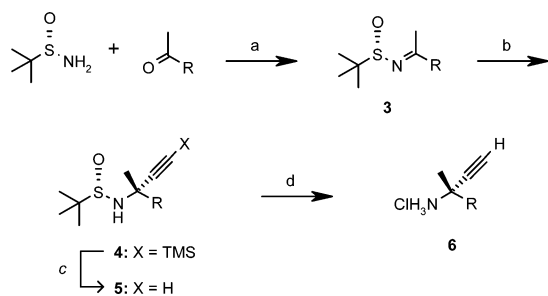


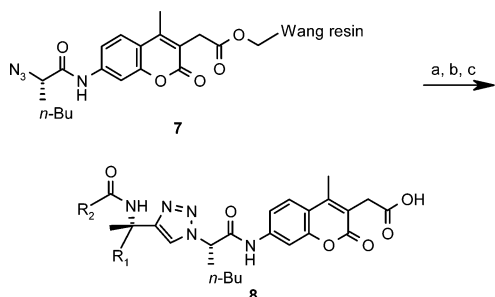
Figure 1. Lead 1,2,3-triazole aldehyde inhibitors identified for cathepsin S.

Scheme 2^a Synthesis of Chiral Propargylamines



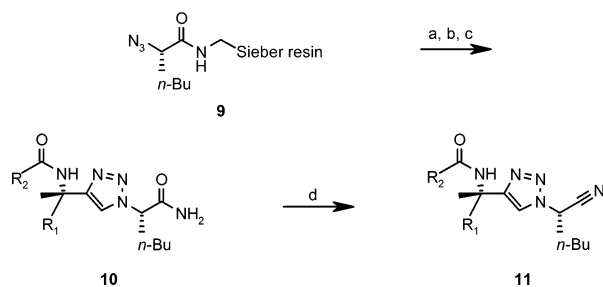
^a Conditions: (a) $\text{Ti}(\text{OEt})_4$, THF, reflux; (b) AlMe_3 , (trimethylsilyl)ethyllithium, -78 °C to rt; (c) TBAF, THF, rt; (d) HCl, CH_3OH , rt.

Scheme 3^a Synthesis of 1,2,3-Triazole Substrates



^a Conditions: (a) **6**, CuI, *i*-Pr₂EtN, THF, rt; (b) $\text{R}_2\text{CO}_2\text{H}$, triphosgene, THF, rt; (c) $\text{CF}_3\text{CO}_2\text{H}$, CH_2Cl_2 , rt.

Scheme 4^a Synthesis of 1,2,3-Triazole Nitrile Inhibitors

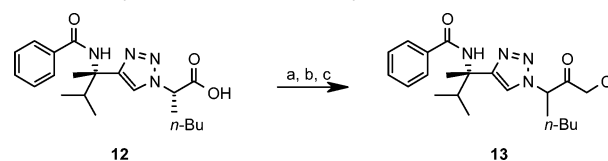


^a Conditions: (a) **6**, CuI, *i*-Pr₂EtN, THF, rt; (b) $\text{R}_2\text{CO}_2\text{H}$, triphosgene, THF, rt; (c) $\text{CF}_3\text{CO}_2\text{H}$, CH_2Cl_2 , rt; (d) 2,4,6-trichlorotriazine, DMF, rt.

For the synthesis of 1,4-disubstituted-1,2,3-triazole-based substrates, the support-bound aminocoumarin acylated with L-norleucine azido acid (**7**) was reacted with chiral propargylamines **6** via a regioselective Cu(I)-catalyzed 1,3-dipolar cycloaddition.¹¹ Acylation of the resulting support-bound α -amino-1,2,3-triazoles, followed by cleavage from the solid support, yielded the 1,2,3-triazole substrates **8** as single diastereomers (Scheme 3).

For the synthesis of 1,4-disubstituted-1,2,3-triazole-based nitrile inhibitors, the chiral propargylamines **6** were reacted with L-norleucine azido acid derivatized Sieber Amide resin **9** to give support-bound 1,2,3-triazole amides (Scheme 4). Acylation of the resulting support-bound α -amino-1,2,3-triazoles, followed by cleavage from the solid support, yielded the 1,2,3-triazole primary amides **10**. Dehydration with 2,4,6-trichlorotriazine then

Scheme 5^a Synthesis of Chloromethyl Ketone Inhibitor **13**



^a Conditions: (a) isobutyl chloroformate, *N*-methylmorpholine, THF, -25 °C; (b) diazomethane, THF, -25 °C; (c) HCl, $\text{CH}_3\text{CO}_2\text{H}$, THF, rt.

Table 1. Inhibition of Cathepsins B, K, L, and S by 1,2,3-Triazole Nitrile Inhibitors

compd	R	K_i (μM)			
		Cat B	Cat K	Cat L	Cat S
11a		$>10^a$	0.88 ± 0.07	$>10^a$	1.2 ± 0.2
11b		$>10^a$	0.43 ± 0.07	$>10^a$	0.42 ± 0.09

^a IC_{50} of inhibitor with enzyme was >10 μM .

produced the desired 1,2,3-triazole nitrile inhibitors **11** as single diastereomers.

The synthesis of chloromethyl ketone inhibitor **13** was accomplished by forming the mixed anhydride of 1,2,3-triazole carboxylic acid **12** and isobutyl chloroformate. Addition of diazomethane to form a diazomethyl ketone, followed by the addition of HCl, yielded chloromethyl ketone **13** as a mixture of diastereomers due to epimerization at the carbon alpha to the ketone during the reaction (Scheme 5).

Results and Discussion

To begin probing the activity of nitrile inhibitors, the nitrile analogues **11a** and **11b** of the most potent aldehyde inhibitors **1** and **2** were assayed against cathepsin S, as well as the related cathepsins B, K, and L (Table 1). Replacing the aldehyde with the nitrile pharmacophore resulted in a ~ 45 -fold drop in potency for compounds **11a** and **11b**. Moreover, compounds **11a** and **11b** selectively inhibited cathepsin S over cathepsins B and L, but no selectivity over cathepsin K was observed. Therefore, the goal of inhibitor optimization was to improve potency and increase selectivity for cathepsin S over cathepsin K.

In collaboration with the Genomics Institute of the Novartis Research Foundation, a crystal structure of the chloromethyl ketone analogue of **1** (compound **13**) in complex with cathepsin S was obtained to guide inhibitor optimization (Figure 2). Crystallographic statistics are summarized in Table 2. Cathepsin S shows a high degree of sequence and structure homology with other cathepsins, including cathepsins B, K, and L. As the functional differences between many of the cathepsins can largely be attributed to tissue distribution, achieving specificity can be challenging. To investigate the binding mode and structural differences between the molecules, the X-ray crystal structure of a complex between cathepsin S and compound **13** was solved in two different crystal forms at 1.5 and 1.9 Å, respectively.^{12,13} The structure of cathepsin S conforms to the canonical papain-like fold consisting of two equal-sized domains, denoted left (L) and right (R), connected by an extensive valley-like cleft containing the catalytic triad, Cys 25, His 164, and Asn 184.¹⁴ The butyl, isopropyl, and benzamide groups of

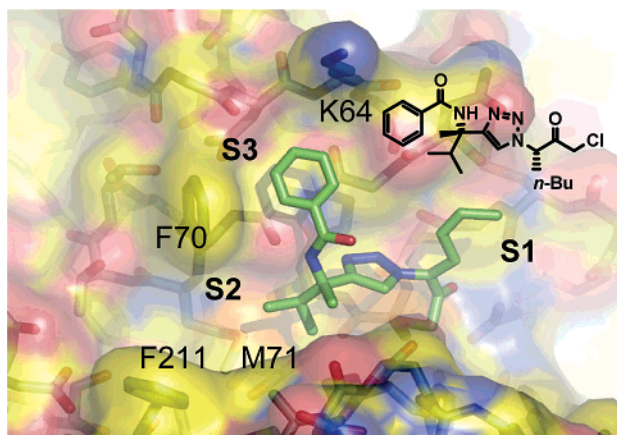


Figure 2. Crystal structure of chloromethyl ketone inhibitor **13** with cathepsin S. The cathepsin S structure is shown as a stick representation above which the semitransparent solvent excluded surface is placed. The atoms are shaded according to element, with the protein carbons colored yellow, the inhibitor carbons are shaded green, nitrogens are blue, and oxygens are red. The figure was produced using Pymol (www.pymol.org).

Table 2. Crystallographic Data for Cathepsin S in Complex with **13**

cathepsin S	crystal form 1	crystal form 2
space group	<i>P</i> 4 ₁ 22	<i>P</i> 6 ₅ 22
unit cell dimensions (Å)		
<i>a</i> = <i>b</i>	85.2	165.9
<i>c</i>	150.8	142.1
wavelength (Å)	1.0	1.0
resolution (Å)	1.5	1.9
outer shell (Å)	1.53–1.48	1.97–1.90
<i>R</i> _{merge} (%) (outer shell)	0.073 (0.642)	0.089 (0.75)
<i>I</i> / <i>sigI</i> (<i>σ</i>) (outer shell)	27.4 (2.2)	28.8 (2.1)
unique refs	92 453	90 365
(obsd)	(422 837)	(526 303)
completeness (%) (outer shell)	99.3 (95.3)	99.7 (100.0)
<i>R</i> _{factor} (<i>R</i> _{free} *) (%)	0.19 (0.20)	0.23 (0.25)
no. protein atoms	3906	5182
no. water atoms	350	369
no. hetero atoms	76	89
rmsd bonds (Å)	0.008	0.014
rmsd bond angles	1.12	1.366
mean <i>B</i> -factor (Å ²)	12.13	25.78

the triazole inhibitor occupy the S₁, S₂, and S₃ enzyme pockets, respectively, and Cys 25 has displaced the chlorine atom of **13** to form a covalent sulfur–carbon bond characteristic of mechanism-based chloromethyl inhibitors of cysteine proteases (Figure 2). The aliphatic P₁ moiety (butyl group) projects into the solvent and does not form close hydrophobic contacts with the surrounding protein. The S₂ binding site is a large pocket lined with hydrophobic residues, while the S₃ binding site is a shallow pocket. The structures of cathepsins K, L, and S are extremely structurally homologous with root-mean-squared deviations (rmsds) of 0.64 and 0.55 Å on 209 and 211 aligned Cα atoms, respectively. Cathepsin B is a more distant homologue but is still very similar, with an rmsd of 1.23 Å on 187 aligned Cα atoms (Figure 3). In general, specificity determinants of the cathepsins are largely confined to the S₁′, S₁, and S₂ pockets, with lesser contributions from the S₃ pocket.

Despite the very high homology across the cathepsin family members, this structure provided valuable insight from which to attain selectivity. The S₃ pocket, occupied by the benzamide moiety, is a small pocket that should not accommodate substitution on the aromatic ring. The flexible nature of Lys 64 (as indicated by the temperature factor for the residue), may allow some movement to accommodate small moieties. Our prior inhibitor SAR verifies this conclusion.¹ In addition, the

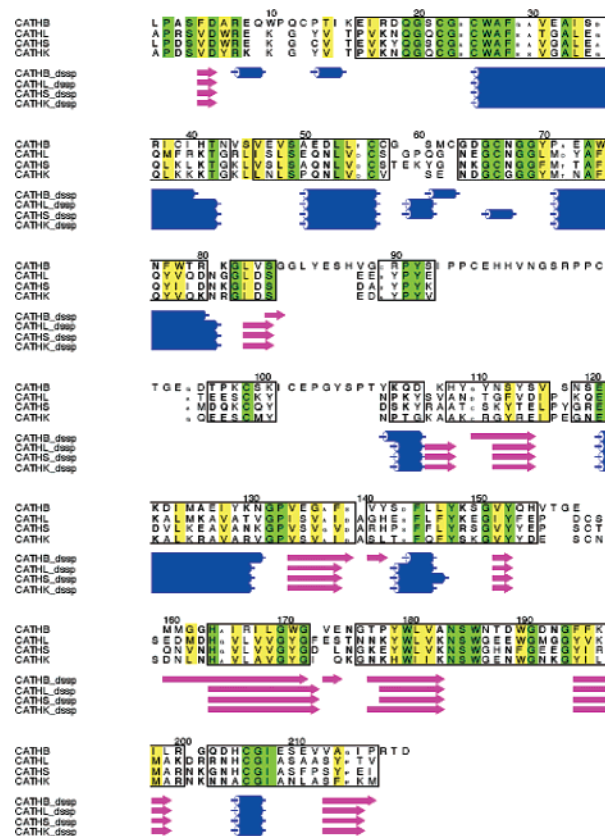


Figure 3. Structural alignment of the cathepsin S structure with cathepsins B, K, and L (PDB entries 1CSB, 1ICF, and 1TU6, respectively). Numbering is according to the cathepsin S structure. Residues colored green are conserved across all cathepsins, while those in yellow are positively conserved. Regions that are boxed are structurally conserved. Alpha helices are represented as blue tubes, while beta sheets are magenta. The figure was produced using STAMP and ALSRCRIP.¹⁵

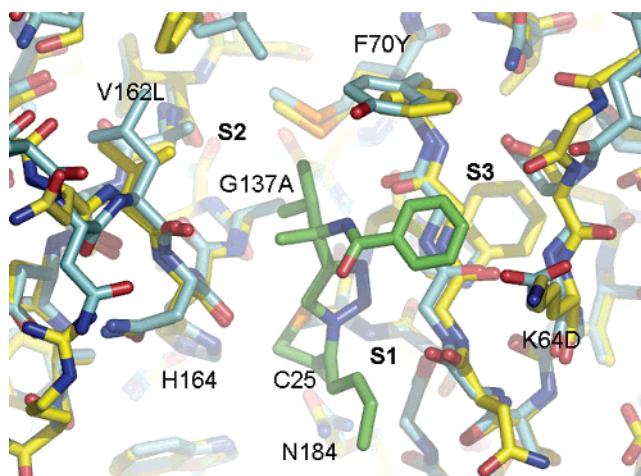
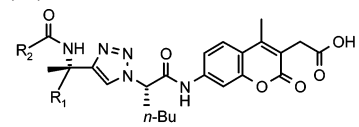


Figure 4. Comparison of specificity pockets with the structure of cathepsin K (PDB ID: 1TU6). Coloring conventions are the same as in Figure 2a, with the exception that the carbons of cathepsin K are shaded cyan.

substitution of negatively charged aspartates and glutamates in structurally identical positions in cathepsins K and L may provide some differential specificity (Figure 4). The S₂ pocket, however, provides the greatest opportunity for achieving selectivity. This pocket is rather large and left unfilled by the isopropyl group. Therefore, replacement of the isopropyl group with larger, extended hydrophobic substituents should result in increased potency as well as selectivity over cathepsin K, which

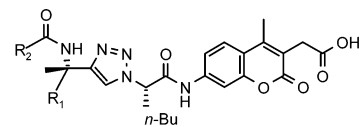
Table 3. Cleavage Efficiencies of 1,2,3-Triazole Substrates with Cathepsins B, K, L, and S


compd	R ₁	R ₂	relative cleavage efficiencies ^a			
			Cat B	Cat K	Cat L	Cat S
8a			0.88	0.016	1.2	1.0
8b			2.2	0.040	0.49	2.4
8c			0.30	0.0039	1.0	3.2
8d			1.2	0.019	0.82	15
8e			0.49	0.0 ^b	0.097	25
8f			0.79	0.0 ^b	0.13	6.3

^a Relative cleavage efficiency values are given as k_{cat}/K_m relative to the activity of substrate **8a** with cathepsin S, which is assigned a value of 1.
^b No activity detected when assayed with [substrate] = 50 μM and [enzyme] = 50 nM.

has a slightly smaller S₂ pocket relative to cathepsin S created by the substitution of larger hydrophobic residues at positions 162 (a leucine instead of a valine) and 137 (an alanine instead of a glycine).¹⁶

As previously reported in the development of inhibitors **1** and **2** (Figure 1), outstanding correlation between substrate-cleavage efficiency and inhibitory activity for the triazole-based substrates and their corresponding mechanism-based inhibitors was observed.² Due to the greater ease of synthesizing and evaluating substrates relative to their corresponding inhibitors, substrate analogues were first prepared to evaluate the effect of introducing larger R₁ substituents on binding and selectivity (Table 3). For substrates with the benzamide moiety, replacement of the isopropyl group (**8a**) with the cyclohexyl group (**8c**) at R₁ resulted in a 3-fold increase in substrate-cleavage efficiency. The same replacement at R₁ with thiophene-containing substrates (**8b–8d**) resulted in a 7-fold increase in activity. In contrast, this substitution resulted in a modest drop in substrate-cleavage efficiency for cathepsins B and K and only a very modest increase for cathepsin L. Further extending the R₁ substituent by introducing 4-methyl substitution on the cyclohexyl ring (**8e** and **8f**) resulted in no detectable substrate cleavage by cathepsin K, with modest reductions also being observed for cathepsins B and L. Moreover, the *trans*-4-methylcyclohexyl substitution, but not the *cis*-4-methylcyclohexyl substitution (**8e** and **8f**, respectively), provided an additional increase in cleavage efficiency by cathepsin S, resulting in an overall 10-fold improvement in cleavage efficiency relative to **8b**, which incorporated an isopropyl group at R₁.

Table 4. Steady State Kinetic Constants for Cathepsin S Acting on 1,2,3-Triazole Substrates


compd	R ₁	R ₂	k_{cat}/K_m (M ⁻¹ s ⁻¹)	k_{cat} (s ⁻¹)	K_m (μM)
8a			1100 ± 100	0.45 ± 0.04	410 ± 40
8b			2600 ± 500	0.77 ± 0.08	300 ± 40
8c			3500 ± 300	0.20 ± 0.01	57 ± 5
8d			17000 ± 800	0.22 ± 0.004	13 ± 0.6
8e			27000 ± 3000	0.46 ± 0.01	17 ± 2

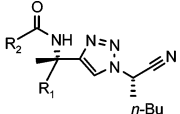
Full enzymatic assay analysis of 1,2,3-triazole substrates (**8a–8e**) with cathepsin S is shown in Table 4. It is interesting that, for this substrate series, the increase in substrate-cleavage efficiency is primarily due to gains in K_m . In the optimization of peptide-based mechanism-based inhibitors, increases in k_{cat} often contribute considerably to increases in substrate-cleavage efficiency, even when modifications are made at sites distant from the mechanism-based pharmacophore.¹⁷ Indeed, in our previously reported optimization of the triazole-based substrates, contributions from both K_m and k_{cat} were observed.¹

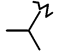
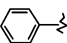
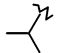
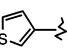
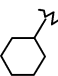
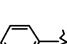
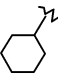
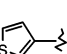
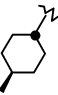
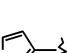
Nitrile inhibitor analogues of compounds **8c**, **8d**, and **8e** were subsequently synthesized (**11c**, **11d**, and **11e**, respectively) and their inhibitory activities toward cathepsins B, K, L, and S were determined (Table 5). The plot of $\log(K_i)$ versus $\log(K_m/k_{\text{cat}})$ for cathepsin S shows excellent correlation between substrate activity and inhibitor potency (Figure 5), which is consistent with transition state theory and with previous correlations between substrates and their corresponding mechanism-based inhibitors.¹⁸

Considerable improvements in both potency and selectivity of cathepsin S inhibitors were achieved upon introducing the *trans*-4-methylcyclohexyl substituent, as predicted by the substrate assay results. Specifically, a 28-fold increase in inhibitor potency against cathepsin S was observed, with **11b** having a K_i of 420 nM and the optimized inhibitor **11e** having a K_i of 15 nM. No significant inhibition of cathepsin B or L was observed when assayed against any of the nitrile inhibitors. Most importantly, the K_i value for **11e** with cathepsin K is significantly greater than 15 μM . Consequently, compound **11e** shows >1000-fold inhibitory selectivity for cathepsin S over all of the closely related human cathepsins that were investigated.

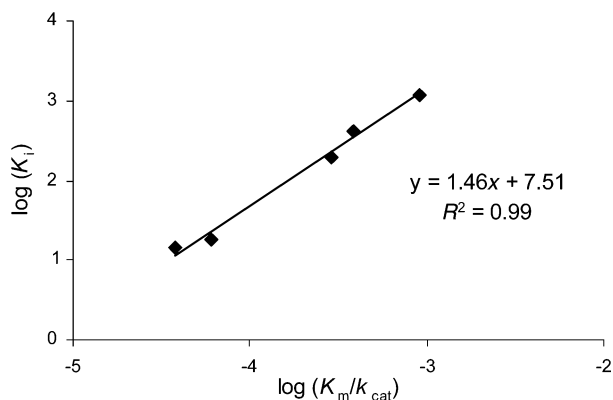
Conclusion

The 1,2,3-triazole nitrile inhibitors **11a** and **11b** were designed based upon the corresponding aldehyde inhibitors **1** and **2** and were determined to have moderate inhibitory activity and poor selectivity for cathepsin S over cathepsin K. A crystal structure

Table 5. Inhibition of Cathepsins B, K, L, and S by 1,2,3-Triazole Nitrile Inhibitors


compd	R ₁	R ₂	K _i (μM)			
			Cat B	Cat K	Cat L	Cat S
11a			>10 ^a	0.88 ± 0.07	>10 ^a	1.2 ± 0.2
11b			>10 ^a	0.43 ± 0.07	>10 ^a	0.42 ± 0.09
11c			>10 ^a	>10 ^a	>10 ^a	0.20 ± 0.02
11d			>10 ^a	1.7 ± 0.1	>10 ^a	0.018 ± 0.003
11e			>15 ^b	>15 ^b	>15 ^b	0.015 ± 0.005

^a IC₅₀ of inhibitor with enzyme is >10 μM. ^b IC₅₀ of inhibitor with enzyme is >15 μM.

**Figure 5.** Plot of log(K_i) vs log(K_m/k_{cat}) for 1,2,3-triazole substrates and corresponding nitrile inhibitors with cathepsin S.

of cathepsin S, irreversibly inhibited by chloromethyl ketone **13**, guided analogue design to improve potency and selectivity. 1,2,3-Triazole substrates **8** were first optimized for cleavage efficiency, followed by the preparation and analysis of inhibitors **11** corresponding to select substrates **8**. The nitrile inhibitor **11e** is a potent (K_i = 15 nM) and low molecular weight (414 Da) nonpeptidic inhibitor of cathepsin S. Additionally, **11e** showed >1000-fold selectivity over cathepsins B, K, and L. These results demonstrate that the SAS method, which entails the identification of novel, low molecular weight nonpeptidic fragments by substrate screening, followed by substrate optimization and conversion to inhibitors, can successfully lead to the development of inhibitors that are novel, potent, and selective.

Experimental Section

General Synthesis Methods. Unless otherwise noted, all reagents were obtained from commercial suppliers and used without purification. THF was distilled under N₂ from sodium/benzophen-

none, and *i*-Pr₂EtN, CH₂Cl₂, pyridine, toluene, Et₂O, and CH₃OH were distilled under N₂ over CaH₂ immediately prior to use. (*S*)-*tert*-Butanesulfinamide was provided by Suven Life Sciences U.S.A., LLC (Monmouth Junction, NJ), and by AllyChem Co., Ltd (Dalian, China). Low amine content DMF was purchased from Acros, Wang resin and Sieber amide resin were purchased from Novabiochem (San Diego, CA), and *O*-(7-azabenzotriazol-1-yl)-*N,N,N',N'*-tetramethyluronium hexafluorophosphate (HATU)⁴ was purchased from PerSeptive Biosystems (Foster City, CA). Fmoc-protected 7-amino-4-methyl coumarin acetic acid (Fmoc-AMCA) was synthesized according to a method analogous to the synthesis of 7-amino-4-carbamoylmethylcoumarin (AMC).¹⁹ Norleucine azide (N₃-Nle-OH) was prepared from L-norleucine, according to literature procedure.²⁰ Compounds **1**, **2**, **8a**, **8b**, **12**, and Fmoc-AMCA-Wang resin were synthesized as previously reported.¹ Compounds **3a–d** and **4a–d** were synthesized according to reported procedures.¹⁰ All solution-phase reactions were carried out in flame-dried glassware under an inert N₂ atmosphere. Normal-phase HPFC purification was carried out on a Biotage SP1 instrument (Charlottesville, VA) equipped with a Biotage Si flash column. Reverse-phase HPLC analysis and purification were conducted with an Agilent 1100 series instrument. Solid-phase reactions were conducted in polypropylene cartridges equipped with 70 mm PE frits (Applied Separations, Allentown, PA) and Teflon stopcocks and rocked on an orbital shaker. ¹H and ¹³C NMR spectra were obtained with Bruker AV-300 and AV-400 spectrometers. Unless otherwise specified, all spectra were obtained in CDCl₃ and chemical shifts are reported in ppm relative to internal CHCl₃. Coupling constants are reported in Hz. Elemental analyses and high-resolution mass spectrometry analyses were performed by the University of California at Berkeley Micro Analysis and Mass spectrometry Facilities.

Synthesis of Propargylamines (Scheme 2). Trimethylsilyl Deprotection (5). To a 0.1 M solution of **4**¹⁰ (1 equiv) in THF cooled in an ice-water bath was added tetrabutylammonium fluoride (TBAF; 3 equiv). The solution was stirred for 2–4 h at room temperature and then the solution was poured into saturated aq NH₄Cl with rapid stirring. The resulting suspension was transferred to a separatory funnel and extracted three times with Et₂O. The combined organic portions were dried (Na₂SO₄), filtered, and concentrated.

(*S,S*)-*N*-(1-Isopropyl-1-methyl-prop-2-ynyl)-2-methylpropanesulfinamide (**5a**). A mixture of 5.10 g of **4a** (17.7 mmol) and 16.8 g of TBAF (53.2 mmol) was reacted in 180 mL of THF. Silica gel chromatography (hexane/EtOAc = 1:1) provided **5a** (3.77 g, 99%) as a white solid: ¹H NMR (400 MHz) δ 0.92 (d, *J* = 6.8 Hz, 3H), 0.95 (d, *J* = 6.8 Hz, 3H), 1.10 (s, 9H), 1.37 (s, 3H), 1.82 (septet, *J* = 6.8 Hz, 1H), 2.37 (s, 1H), 3.18 (s, 1H); ¹³C NMR (100 MHz) δ 16.9, 17.4, 22.3, 25.0, 38.1, 55.8, 56.6, 72.8, 85.8. HRMS (FAB⁺) *m/z*: (MH⁺) calcd for C₁₁H₂₂NOS, 216.1422; found, 216.1421.

(*S,S*)-*N*-(1-Cyclohexyl-1-methyl-prop-2-ynyl)-2-methylpropanesulfinamide (**5b**). A mixture of 2.73 g of **4b** (8.34 mmol) and 7.89 g of TBAF (25.0 mmol) was reacted in 83 mL of THF. HPFC purification (hexane/EtOAc = 94:6 for 3 min, 94:6 to 50:50 over 33 min) provided **5b** (1.58 g, 74%) as a white solid: ¹H NMR (400 MHz) δ 0.99–1.27 (m, 5H), 1.17 (s, 9H), 1.44 (s, 3H), 1.47–1.55 (m, 1H), 1.62–1.68 (m, 1H), 1.75–1.82 (m, 2H), 1.87–1.97 (m, 2H), 2.43 (s, 1H), 3.24 (s, 1H); ¹³C NMR (100 MHz) δ 22.5, 25.5, 26.17, 26.24, 27.0, 27.6, 48.2, 55.9, 56.5, 73.0, 86.3. HRMS (FAB⁺) *m/z*: (MH⁺) calcd for C₁₄H₂₆NOS, 256.1735; found, 256.1728.

(*S,S*)-*N*-[1-Methyl-1-(*trans*-4-methyl-cyclohexyl)-prop-2-ynyl]-2-methylpropanesulfinamide (**5c**). A mixture of 0.69 g of **4c** (2.0 mmol) and 1.6 g of TBAF (6.1 mmol) was reacted in 20 mL of THF. HPFC purification (hexane/EtOAc = 94:6 for 3 min, 94:6 to

^a Abbreviation: AMC, 7-amino-4-carbamoylmethylcoumarin; AMCA, 7-amino-4-methyl coumarin acetic acid; E-64, *L*-*trans*-epoxysuccinyl-Leu-4-guanidinobutylamide; E-64c, *L*-*trans*-epoxysuccinyl-Leu-3-methylbutylamide; HATU, *O*-(7-azabenzotriazol-1-yl)-*N,N,N',N'*-tetra-methyluronium hexafluorophosphate; HPFC, high-performance flash chromatography.

50:50 over 33 min) provided **5c** (0.53 g, 97%) as a white solid: $^1\text{H NMR}$ (400 MHz) δ 0.85 (d, $J = 6.4$ Hz, 3H), 0.87–0.96 (m, 2H), 1.06–1.34 (m, 3H), 1.18 (s, 9H), 1.44 (s, 3H), 1.44–1.52 (m, 1H), 1.70–1.77 (m, 2H), 1.86–1.96 (m, 2H), 2.43 (s, 1H), 3.25 (s, 1H); $^{13}\text{C NMR}$ (100 MHz) δ 22.3, 22.5, 25.7, 26.8, 27.5, 32.5, 34.8, 47.9, 55.9, 56.4, 73.0, 86.33. HRMS (FAB⁺) m/z : (MH⁺) calcd for C₁₅H₂₈NOS, 270.1892; found, 270.1890.

(Ss,S)-*N*-[1-Methyl-1-(*cis*-4-methyl-cyclohexyl)-prop-2-ynyl]-2-methylpropanesulfonamide (**5d**). A mixture of 1.0 g of **4d** (2.9 mmol) and 2.3 g of TBAF (8.8 mmol) was reacted in 29 mL of THF. HPFC purification (hexane/EtOAc = 94:6 for 3 min, 94:6 to 50:50 over 33 min) provided **5d** (0.78 g, 99%) as a white solid: $^1\text{H NMR}$ (400 MHz) δ 0.94 (d, $J = 7.6$ Hz, 3H), 1.20 (s, 9H), 1.31–1.44 (m, 2H), 1.46–1.60 (m, 8H), 1.62–1.72 (m, 2H), 1.90–1.98 (m, 1H), 2.46 (s, 1H), 3.27 (s, 1H); $^{13}\text{C NMR}$ (100 MHz) δ 17.3, 20.9, 21.5, 22.5, 25.7, 26.6, 31.50, 31.53, 48.4, 56.0, 56.6, 73.0, 86.3. HRMS (FAB⁺) m/z : (MH⁺) calcd for C₁₅H₂₈NOS, 270.1892; found, 270.1893.

Sulfinyl Cleavage (6). To a 0.15 M solution of **5** (1 equiv) in CH₃OH was added HCl (3 equiv) as a 4 M solution in 1,4-dioxane. The solution was stirred for 1–2 h and concentrated to yield **6**, the propargylamine hydrochloride salts.

(S)-1-Isopropyl-1-methyl-prop-2-ynylamine Hydrochloride (**6a**). A mixture of 3.77 g of **5a** (17.5 mmol) and 13.0 mL of 4 M HCl in dioxane (52.5 mmol) was reacted in 120 mL of CH₃OH to afford propargylamine **6a** (2.55 g, 99%) as a white solid: $^1\text{H NMR}$ (CD₃OD, 400 MHz) δ 0.93 (d, $J = 6.8$ Hz, 3H), 0.97 (d, $J = 6.8$ Hz, 3H), 1.60 (s, 3H), 2.10 (septet, $J = 6.8$ Hz, 1H), 3.30 (s, 1H); $^{13}\text{C NMR}$ (CD₃OD, 100 MHz) δ 17.8, 17.9, 24.5, 37.7, 56.9, 78.1, 81.5. HRMS (FAB⁺) m/z : (MH⁺) calcd for C₇H₁₄N, 112.1126; found, 112.1125.

(S)-1-Cyclohexyl-1-methyl-prop-2-ynylamine Hydrochloride (**6b**). A mixture of 1.58 g of **5b** (6.19 mmol) and 4.75 mL of 4 M HCl in dioxane (19.0 mmol) was reacted in 41 mL of CH₃OH to afford propargylamine **6b** (1.15 g, 99%) as a white solid: $^1\text{H NMR}$ (CD₃OD, 400 MHz) δ 1.15–1.40 (m, 5H), 1.61 (s, 3H), 1.65–1.78 (m, 2H), 1.82–1.96 (m, 4H), 3.32 (s, 1H); $^{13}\text{C NMR}$ (CD₃OD, 100 MHz) δ 24.6, 26.97, 27.01, 27.1, 28.3, 28.5, 47.1, 56.3, 78.0, 82.0. HRMS (FAB⁺) m/z : (MH⁺) calcd for C₁₀H₁₈N, 152.1439; found, 152.1443.

(S)-1-Methyl-1-(*trans*-4-methyl-cyclohexyl)-prop-2-ynylamine Hydrochloride (**6c**). A mixture of 0.37 g of **5c** (1.4 mmol) and 1.0 mL of 4 M HCl in dioxane (4.1 mmol) was reacted in 9 mL of CH₃OH to afford propargylamine **6c** (0.27 g, 96%) as a white solid: $^1\text{H NMR}$ (CD₃OD, 400 MHz) δ 0.92 (d, $J = 6.4$ Hz, 3H), 0.94–1.06 (m, 2H), 1.23–1.41 (m, 3H), 1.59 (s, 3H), 1.60–1.69 (m, 1H), 1.80–1.95 (m, 4H), 3.29 (s, 1H); $^{13}\text{C NMR}$ (CD₃OD, 100 MHz) δ 22.8, 24.7, 28.2, 28.4, 33.5, 35.58, 35.64, 46.8, 56.2, 78.1, 82.0. HRMS (FAB⁺) m/z : (MH⁺) calcd for C₁₁H₂₀N, 166.1596; found, 166.1590.

(S)-1-Methyl-1-(*cis*-4-methyl-cyclohexyl)-prop-2-ynylamine Hydrochloride (**6d**). A mixture of 0.75 g of **5d** (2.8 mmol) and 2.1 mL of 4 M HCl in dioxane (8.3 mmol) was reacted in 19 mL of CH₃OH to afford propargylamine **6d** (0.55 g, 97%) as a white solid: $^1\text{H NMR}$ (CD₃OD, 400 MHz) δ 0.89 (d, $J = 7.6$ Hz, 3H), 1.31–1.59 (m, 12H), 1.83–1.92 (m, 1H), 3.20 (s, 1H); $^{13}\text{C NMR}$ (CD₃OD, 100 MHz) δ 17.6, 22.3, 22.4, 24.7, 27.8, 32.2, 32.3, 47.3, 56.3, 78.0, 81.9. HRMS (FAB⁺) m/z : (MH⁺) calcd for C₁₁H₂₀N, 166.1596; found, 166.1593.

Synthesis of 1,4-Disubstituted-1,2,3-triazole AMCA Substrates (Scheme 3). Synthesis of N₃-Nle-AMCA-Wang Resin (7). A 20% solution of piperidine in DMF (30 mL) was added to a cartridge containing Fmoc-AMCA-Wang resin (4.3 g, 0.49 mmol/g). The mixture was shaken for 5 min, the solution was removed, and the resin was washed with DMF (30 mL). The process was repeated once, and the resin was washed with three portions of DMF (30 mL). A 0.4 M solution of HATU (4.0 g, 11 mmol) in 26 mL of DMF with collidine (1.4 mL, 11 mmol) and N₃-Nle-OH (1.7 g, 11 mmol) was added to the resin, and the mixture was shaken for 48 h. After removal of the solution, the resin was washed with three portions (30 mL) each of DMF, THF, CH₃OH, THF, and

CH₂Cl₂, and the solvent was removed in vacuo. Resin **7** was stored at –20 °C until further use.

General Synthesis of Substrates (8). To resin **7** (0.60–0.66 mmol/g, 1 equiv), preswollen in THF, was added a 0.02 M solution of propargylamine **6** (1–2 equiv) in THF, with *i*-Pr₂EtN (100 equiv) and CuI (3 equiv). The mixture was shaken for 20–48 h. After removal of the solution, the resin was washed with three portions (20 mL) each of THF, CH₃OH, CH₃CN, and THF. After solvent removal, *i*-Pr₂EtN (8 equiv) was added to the derivatized resin. To a 0.1 M solution of carboxylic acid (3.5 equiv) in THF with triphosgene (1.1 equiv) was added 2,4,6-collidine (10 equiv). The resulting slurry was stirred for about 1 min and then added to the cartridge containing the derivatized resin. The resulting mixture was shaken for 4–12 h. After removal of the solution, the resin was washed with THF (20 mL) and the coupling was repeated two more times. After removal of the solution, the resin was washed with three portions (20 mL) each of THF, CH₃OH, THF, and CH₂Cl₂, and then the product was cleaved from the solid support [see general procedure for cleavage]. The crude product mixture was purified by HPLC [preparatory reverse-phase C18 column (24.1 × 250 mm), CH₃CN/H₂O–0.1% CF₃CO₂H = 5:95 over 50 min; 10 mL/min; 254 nm detection for 60 min], extracted into EtOAc, dried (Na₂SO₄), filtered, and concentrated. Due to the presence of CF₃CO₂H in the purification solvents, AMCA substrates, **8**, were isolated with 0–1 equiv of CF₃CO₂H (by $^1\text{H NMR}$). Purity of all substrate products was determined to be >95%, analyzed by HPLC.

General Procedure for Support Cleavage. The resin was swollen in CH₂Cl₂. To the swollen resin was added a solution of 9:1 CH₂Cl₂/95% CF₃CO₂H, 2.5% H₂O, 2.5% triisopropylsilane, and the mixture was shaken for 1–2 h. Upon removal of the solution, the resin was washed with one portion of the cleavage solution and three portions of CH₂Cl₂. The combined washes were concentrated under reduced pressure.

Substrate 8c. A mixture of 75 mg of propargylamine **6b** (0.40 mmol), 0.19 g of CuI (1.0 mmol), and 6.0 mL of *i*-Pr₂EtN (33 mmol) in 34 mL of THF was added to 0.50 g of resin **7** (0.33 mmol). The support-bound amine intermediate was then acylated using 0.15 g of benzoic acid (1.2 mmol), 0.11 g of triphosgene (0.36 mmol), 0.44 mL of 2,4,6-collidine (3.3 mmol), and 0.45 mL of *i*-Pr₂EtN (2.6 mmol) in 12 mL of THF. Preparative HPLC purification gave 30 mg of **8c** (14%) as a sticky yellow solid: $^1\text{H NMR}$ (DMSO-*d*₆, 400 MHz) δ 0.76–1.36 (m, 12H), 1.42–1.50 (m, 1H), 1.54–1.66 (m, 2H), 1.68–1.75 (m, 1H), 1.76 (s, 3H), 1.82–1.89 (m, 1H), 2.12–2.24 (m, 2H), 2.26–2.33 (m, 1H), 2.34 (s, 3H), 3.52 (s, 2H), 5.52 (dd, $J = 7.0, 9.2$ Hz, 1H), 7.41–7.46 (m, 2H), 7.47–7.53 (m, 2H), 7.73–7.79 (m, 4H), 8.05 (s, 1H), 8.13 (s, 1H), 11.28 (s, 1H); $^{13}\text{C NMR}$ (DMSO-*d*₆, 100 MHz) δ 13.7, 14.9, 20.8, 21.5, 26.1, 26.2, 27.0, 27.2, 27.4, 31.6, 33.7, 45.0, 57.4, 63.4, 106.0, 115.7, 116.1, 119.3, 121.7, 126.1, 127.3, 128.1, 130.9, 135.7, 140.9, 148.0, 150.9, 152.2, 160.9, 166.1, 167.5, 171.9. HRMS (FAB⁺) m/z : (MH⁺) calcd for C₃₅H₄₂N₅O₆, 628.3135; found, 628.3145.

Substrate 8d. A mixture of 56 mg of propargylamine **6b** (0.30 mmol), 0.11 g of CuI (0.58 mmol), and 5.2 mL of *i*-Pr₂EtN (30 mmol) in 15 mL of THF was added to 0.34 g of resin **7** (0.20 mmol). The support-bound amine intermediate was then acylated using 90 mg of thiophene-3-carboxylic acid (0.70 mmol), 65 mg of triphosgene (0.22 mmol), 0.26 mL of 2,4,6-collidine (2.0 mmol), and 0.28 mL of *i*-Pr₂EtN (1.6 mmol) in 7 mL of THF. Preparative HPLC purification gave 66 mg of **8d** (52%) as a sticky yellow solid: $^1\text{H NMR}$ (DMSO-*d*₆, 400 MHz) δ 0.78–1.36 (m, 12H), 1.38–1.44 (m, 1H), 1.55–1.66 (m, 2H), 1.68–1.74 (m, 4H), 1.80–1.87 (m, 1H), 2.11–2.24 (m, 2H), 2.25–2.34 (m, 1H), 2.37 (s, 3H), 3.59 (s, 2H), 5.47 (dd, $J = 6.6, 9.0$ Hz, 1H), 7.44 (dd, $J = 1.2, 5.2$ Hz, 1H), 7.49–7.55 (m, 2H), 7.75 (d, $J = 2.0$ Hz, 1H), 7.79–7.83 (m, 2H), 8.10 (s, 1H), 8.16 (dd, $J = 1.2, 2.8$ Hz), 11.12 (s, 1H), 12.55 (br s, 1H); $^{13}\text{C NMR}$ (DMSO-*d*₆, 100 MHz) δ 13.7, 14.9, 20.7, 21.5, 26.1, 26.2, 26.9, 27.2, 27.5, 31.6, 32.9, 45.0, 57.3, 63.4, 106.0, 115.7, 115.9, 118.3, 118.8, 121.7, 126.3, 127.2, 128.5,

138.6, 141.0, 148.6, 151.0, 152.2, 160.8, 161.7, 167.5, 171.4. HRMS (FAB⁺) *m/z*: (MH⁺) calcd for C₃₃H₄₀N₅O₆S, 634.2699; found, 634.2682.

Substrate 8e. A mixture of 61 mg of propargylamine **6c** (0.30 mmol), 0.11 g of CuI (0.58 mmol), and 5.2 mL of *i*-Pr₂EtN (30 mmol) in 15 mL of THF was added to 0.34 g of resin **7** (0.20 mmol). The support-bound amine intermediate was then acylated using 90 mg of thiophene-3-carboxylic acid (0.70 mmol), 65 mg of triphosgene (0.22 mmol), 0.26 mL of 2,4,6-collidine (2.0 mmol), and 0.28 mL of *i*-Pr₂EtN (1.6 mmol) in 7 mL of THF. Preparative HPLC purification gave 48 mg of **8e** (37%) as a sticky yellow solid: ¹H NMR (DMSO-*d*₆, 400 MHz) δ 0.74–0.85 (m, 7H), 0.85–1.34 (m, 8H), 1.36–1.44 (m, 1H), 1.55–1.63 (m, 1H), 1.65–1.71 (m, 1H), 1.73 (s, 3H), 1.78–1.84 (m, 1H), 2.09–2.28 (m, 3H), 2.31 (s, 3H), 3.41 (s, 2H), 5.47–5.54 (m, 1H), 7.44 (dd, *J* = 1.2, 5.2 Hz, 1H), 7.48 (dd, *J* = 2.0, 8.8 Hz, 1H), 7.54 (dd, *J* = 2.8, 5.2 Hz, 1H), 7.68–7.72 (m, 2H), 7.82 (s, 1H), 8.11 (s, 1H), 8.17 (dd, *J* = 1.2, 2.8 Hz, 1H), 11.34 (s, 1H); ¹³C NMR (DMSO-*d*₆, 100 MHz) δ 14.2, 15.3, 21.2, 21.9, 22.9, 27.1, 27.4, 27.9, 32.0, 32.7, 35.3, 35.7, 45.1, 57.7, 63.7, 106.4, 116.0, 116.8, 121.4, 122.2, 126.2, 126.8, 127.7, 129.0, 139.0, 140.9, 147.3, 151.4, 152.5, 161.5, 162.1, 167.9, 173.0. HRMS (FAB⁺) *m/z*: (MH⁺) calcd for C₃₄H₄₂N₅O₆S, 648.2856; found, 648.2855.

Substrate 8f. A mixture of 61 mg of propargylamine **6d** (0.30 mmol), 0.11 g of CuI (0.58 mmol), and 5.2 mL of *i*-Pr₂EtN (30 mmol) in 15 mL of THF was added to 0.34 g of resin **7** (0.20 mmol). The support-bound amine intermediate was then acylated using 90 mg of thiophene-3-carboxylic acid (0.70 mmol), 65 mg of triphosgene (0.22 mmol), 0.26 mL of 2,4,6-collidine (2.0 mmol), and 0.28 mL of *i*-Pr₂EtN (1.6 mmol) in 7 mL of THF. Preparative HPLC purification gave 72 mg of **8f** (56%) as a sticky yellow solid: ¹H NMR (DMSO-*d*₆, 400 MHz) δ 0.77 (d, *J* = 7.2 Hz, 3H), 0.81 (t, *J* = 7.2 Hz, 3H), 0.93–1.62 (m, 12H), 1.76 (s, 3H), 1.80–1.88 (m, 1H), 2.13–2.30 (m, 3H), 2.32 (s, 3H), 3.47 (s, 2H), 5.48–5.54 (m, 1H), 7.44 (d, *J* = 1.2, 5.2 Hz, 1H), 7.49 (dd, *J* = 1.8, 8.4 Hz, 1H), 7.54 (dd, *J* = 2.8, 5.2 Hz, 1H), 7.71–7.76 (m, 2H), 7.83 (s, 1H), 8.12 (s, 1H), 8.16 (dd, *J* = 1.2, 2.8 Hz, 1H), 11.27 (s, 1H); ¹³C NMR (DMSO-*d*₆, 100 MHz) δ 14.2, 15.3, 17.5, 21.1, 21.3, 21.5, 21.9, 26.7, 27.9, 31.9, 34.8, 45.6, 57.9, 63.8, 106.4, 116.0, 116.6, 120.4, 122.2, 126.4, 126.8, 127.6, 129.0, 139.1, 141.2, 148.0, 151.1, 152.5, 161.4, 162.1, 167.9, 172.7. HRMS (FAB⁺) *m/z*: (MH⁺) calcd for C₃₄H₄₂N₅O₆S, 648.2856; found, 648.2849.

Synthesis of 1,4-Disubstituted-1,2,3-triazole Inhibitors (Scheme 4). **Synthesis of N₃-Nle-Sieber Amide Resin (9).** A 20% solution of piperidine in DMF (30 mL) was added to a cartridge containing Sieber Amide resin (1.9 g, 100–200 mesh, 0.52 mmol/g). The mixture was shaken for 5 min, the solution was removed, and the resin was washed with DMF (30 mL). The process was repeated once, and the resin was washed with three portions of DMF (30 mL). A 0.4 M solution of HATU (1.9 g, 5.0 mmol) in 13 mL of DMF with collidine (0.66 mL, 5.0 mmol) and N₃-Nle-OH (0.79 g, 5.0 mmol) was added to the resin, and the mixture was shaken for 48 h. After removal of the solution, the resin was washed with three portions (30 mL) each of DMF, THF, CH₃OH, THF, and CH₂Cl₂, and the solvent was removed in vacuo. Resin **9** was stored at –20 °C until further use.

General Synthesis of Primary Amides (10). To resin **9** (0.83 mmol/g, 1 equiv), preswollen in THF, was added a 0.02 M solution of propargylamine **6** (1–2 equiv) in THF, with *i*-Pr₂EtN (100 equiv) and CuI (3 equiv). The mixture was shaken for 20–48 h. After removal of the solution, the resin was washed with three portions (20 mL) each of THF, CH₃OH, CH₃CN, and THF. After solvent removal, *i*-Pr₂EtN (8 equiv) was added to the derivatized resin. To a 0.1 M solution of carboxylic acid (3–5 equiv) in THF with triphosgene (1.1 equiv) was added 2,4,6-collidine (10 equiv). The resulting slurry was stirred for about 1 min and then added to the cartridge containing the derivatized resin. The resulting mixture was shaken for 4–12 h. After removal of the solution, the resin was washed once with THF (20 mL), and the coupling was repeated two more times. After removal of the solution, the resin was washed with three portions (20 mL) each of THF, CH₃OH, THF, and CH₂-

Cl₂, and then the product was cleaved from the solid support [see general procedure for cleavage]. Primary amides, **10**, were purified by silica gel chromatography (hexane/EtOAc = 1:7) or by HPFC (hexane/EtOAc = 88:12 for 2 min, 88:12 to 0:100 over 19 min).

Amide 10a. A mixture of 0.11 g of propargylamine **6a** (0.75 mmol), 0.29 g of CuI (1.5 mmol), and 8.7 mL of *i*-Pr₂EtN (50 mmol) in 38 mL of THF was added to 0.42 g of resin **9** (0.50 mmol). The support-bound amine intermediate was then acylated using 0.21 g of benzoic acid (1.8 mmol), 0.16 g of triphosgene (0.55 mmol), 0.66 mL of 2,4,6-collidine (5.0 mmol), and 0.70 mL of *i*-Pr₂EtN (4.0 mmol) in 18 mL of THF. HPFC purification provided **10a** (62 mg, 33%) as a yellow solid: ¹H NMR (400 MHz) δ 0.79–0.88 (m, 6H), 0.97 (d, *J* = 6.8 Hz, 3H), 1.06–1.16 (m, 1H), 1.20–1.38 (m, 3H), 1.88 (s, 3H), 2.10–2.28 (m, 2H), 2.85 (septet, *J* = 6.8 Hz, 1H), 5.09 (dd, *J* = 6.0, 9.6 Hz, 1H), 6.12 (br s, 1H), 6.63 (br s, 1H), 7.19 (s, 1H), 7.38–7.42 (m, 2H), 7.47 (t, *J* = 7.2 Hz, 1H), 7.74 (d, *J* = 7.6 Hz, 1H), 7.78 (s, 1H); ¹³C NMR (100 MHz) δ 13.7, 17.3, 17.6, 21.4, 21.9, 27.9, 32.4, 34.9, 58.3, 64.4, 122.3, 126.8, 128.6, 131.4, 135.2, 150.7, 166.9, 170.8. HRMS (FAB⁺) *m/z*: (MH⁺) calcd for C₂₀H₃₀N₅O₂, 372.2400; found, 372.2393.

Amide 10b. A mixture of 0.30 g of propargylamine **6a** (2.0 mmol), 0.57 g of CuI (3.0 mmol), and 17 mL of *i*-Pr₂EtN (100 mmol) in 100 mL of THF was added to 0.90 g of resin **9** (0.50 mmol). The support-bound amine intermediate was then acylated using 0.64 g of thiophene-3-carboxylic acid (5.0 mmol), 0.33 g of triphosgene (1.1 mmol), 1.3 mL of 2,4,6-collidine (10 mmol), and 1.4 mL of *i*-Pr₂EtN (8.0 mmol) in 50 mL of THF. Chromatography provided **10b** (144 mg, 38%) as a yellow solid: ¹H NMR (400 MHz) δ 0.77 (d, *J* = 6.8 Hz, 3H), 0.81 (t, *J* = 7.0 Hz, 3H), 0.93 (d, *J* = 6.8 Hz, 3H), 1.03–1.15 (m, 1H), 1.16–1.35 (m, 3H), 1.84 (s, 3H), 2.02–2.25 (m, 2H), 2.79 (septet, *J* = 6.8 Hz, 1H), 5.19 (dd, *J* = 6.2, 9.4 Hz, 1H), 6.45 (br s, 1H), 7.00 (br s, 1H), 7.24–7.28 (m, 2H), 7.37 (dd, *J* = 1.2, 5.2 Hz, 1H), 7.78 (s, 1H), 7.85 (dd, *J* = 1.2, 3.0 Hz, 1H); ¹³C NMR (100 MHz) δ 13.6, 17.2, 17.5, 21.3, 21.8, 27.7, 32.4, 34.9, 58.2, 64.0, 121.7, 126.1, 126.3, 128.0, 138.2, 150.6, 162.4, 170.7; HRMS (FAB⁺) *m/z*: (MH⁺) calcd for C₁₈H₂₈N₅O₂S, 378.1964; found, 378.1961.

Amide 10c. A mixture of 0.38 g of propargylamine **6b** (2.0 mmol), 0.57 g of CuI (3.0 mmol), and 17 mL of *i*-Pr₂EtN (100 mmol) in 100 mL of THF was added to 0.83 g of resin **9** (1.0 mmol). The support-bound amine intermediate was then acylated using 0.43 g of benzoic acid (3.5 mmol), 0.33 g of triphosgene (1.1 mmol), 1.3 mL of 2,4,6-collidine (10 mmol), and 1.4 mL of *i*-Pr₂EtN (8.0 mmol) in 35 mL of THF. Chromatography provided **10c** (147 mg, 37%) as a yellow solid: ¹H NMR (400 MHz) δ 0.76–1.39 (m, 12H), 1.56–1.84 (m, 5H), 1.87 (s, 3H), 2.05–2.25 (m, 2H), 2.33–2.42 (m, 1H), 5.13 (app t, *J* = 7.6 Hz, 1H), 6.39 (br s, 1H), 6.93 (br s, 1H), 7.31 (s, 1H), 7.38 (app t, *J* = 7.4 Hz, 2H), 7.45 (t, *J* = 7.4 Hz, 1H), 7.74 (d, *J* = 7.6 Hz, 2H), 7.76 (s, 1H); ¹³C NMR (100 MHz) δ 13.7, 21.7, 21.9, 26.2, 26.3, 27.5, 27.8, 32.4, 45.3, 58.0, 64.1, 122.1, 126.8, 128.5, 131.4, 135.2, 151.0, 166.9, 171.0. HRMS (FAB⁺) *m/z*: (MH⁺) calcd for C₂₃H₃₄N₅O₂, 412.2713; found, 412.2703.

Amide 10d. A mixture of 0.38 g of propargylamine **6b** (2.0 mmol), 0.57 g of CuI (3.0 mmol), and 17 mL of *i*-Pr₂EtN (100 mmol) in 100 mL of THF was added to 0.90 g of resin **9** (0.50 mmol). The support-bound amine intermediate was then acylated using 0.64 g of thiophene-3-carboxylic acid (5.0 mmol), 0.33 g of triphosgene (1.1 mmol), 1.3 mL of 2,4,6-collidine (10 mmol), and 1.4 mL of *i*-Pr₂EtN (8.0 mmol) in 50 mL of THF. Chromatography provided **10d** (72 mg, 17%) as a yellow solid: ¹H NMR (400 MHz) δ 0.72–1.03 (m, 6H), 1.08–1.40 (m, 6H), 1.58–1.85 (m, 5H), 1.88 (s, 3H), 2.12–2.20 (m, 1H), 2.23–2.34 (m, 1H), 2.38–2.47 (m, 1H), 5.09 (dd, *J* = 6.0, 9.2 Hz, 1H), 5.86 (br s, 1H), 6.49 (br s, 1H), 7.14 (s, 1H), 7.28–7.34 (m, 1H), 7.38 (d, *J* = 5.2 Hz, 1H), 7.66 (s, 1H), 7.85 (d, *J* = 2.0 Hz, 1H); ¹³C NMR (100 MHz) δ 13.7, 21.9, 22.3, 26.29, 26.32, 26.4, 27.68, 27.71, 27.9, 32.5, 45.1, 58.2, 64.6, 121.9, 126.1, 126.4, 127.9, 138.5, 151.2, 162.2, 170.4. HRMS (FAB⁺) *m/z*: (MH⁺) calcd for C₂₁H₃₂N₅O₂S, 418.2276; found, 418.2275.

Amide 10e. A mixture of 0.15 g of propargylamine **6c** (0.75 mmol), 0.29 g of CuI (1.5 mmol), and 8.7 mL of *i*-Pr₂EtN (50 mmol) in 38 mL of THF was added to 0.42 g of resin **9** (0.50 mmol). The support-bound amine intermediate was then acylated using 0.22 g of thiophene-3-carboxylic acid (1.8 mmol), 0.16 g of triphosgene (0.55 mmol), 0.66 mL of 2,4,6-collidine (5.0 mmol), and 0.70 mL of *i*-Pr₂EtN (4.0 mmol) in 18 mL of THF. HPFC purification provided **10e** (70 mg, 32%) as a yellow solid: ¹H NMR (400 MHz) δ 0.77–0.85 (m, 6H), 0.86–1.05 (m, 4H), 1.06–1.36 (m, 5H), 1.54–1.76 (m, 3H), 1.79–1.87 (m, 4H), 2.12–2.27 (m, 2H), 2.28–2.37 (m, 1H), 5.04–5.13 (m, 1H), 6.40 (br s, 1H), 6.80 (br s, 1H), 7.04 (s, 1H), 7.27–7.33 (m, 2H), 7.77–7.84 (m, 2H); ¹³C NMR (100 MHz) δ 13.7, 21.6, 21.9, 22.3, 27.3, 27.5, 27.9, 32.3, 32.6, 34.8, 34.9, 45.0, 57.9, 64.3, 122.7, 125.9, 126.5, 128.5, 137.9, 151.0, 162.6, 171.8. HRMS (FAB⁺) *m/z*: (MH⁺) calcd for C₂₂H₃₄N₅O₂S, 432.2433; found, 432.2428.

General Synthesis of Nitrile Inhibitors (11). A 0.15 M solution of amide **10** (1 equiv) in DMF was cooled in an ice–water bath and 2,4,6-trichlorotriazine (1 equiv) was added. The solution was stirred for 2 h at room temperature before being added to 25 mL of EtOAc. The solution was transferred to a separatory funnel and washed three times with H₂O, dried (Na₂SO₄), filtered, and concentrated. The inhibitors, **11**, were purified by HPLC [preparatory reverse-phase C18 column (24.1 × 250 mm), CH₃CN/H₂O–0.1% CF₃CO₂H = 5:95 over 50 min; 10 mL/min; 254 nm detection for 60 min] or by HPFC (hexane/EtOAc = 94:6 for 1 min, 94:6 to 0:100 over 10 min).

Inhibitor 11a. A mixture of 45 mg of amide **10a** (0.12 mmol) and 22 mg of 2,4,6-trichlorotriazine (0.12 mmol) was reacted in 0.8 mL of DMF. HPFC purification provided **11a** (27 mg, 64%) as a yellow solid: ¹H NMR (400 MHz) δ 0.81 (d, *J* = 6.8 Hz, 3H), 0.91 (t, *J* = 7.0 Hz, 3H), 0.97 (d, *J* = 6.8 Hz, 3H), 1.33–1.49 (m, 4H), 1.89 (s, 3H), 2.19–2.33 (m, 2H), 2.90 (septet, *J* = 6.8 Hz, 1H), 5.52 (app t, *J* = 7.6 Hz, 1H), 7.11 (s, 1H), 7.38–7.44 (m, 2H), 7.45–7.51 (m, 1H), 7.74–7.79 (m, 3H); ¹³C NMR (100 MHz) δ 13.6, 17.3, 17.5, 21.4, 21.6, 27.2, 34.1, 34.8, 51.1, 58.3, 115.5, 120.5, 126.8, 128.5, 131.4, 135.3, 151.7, 166.6. HRMS (FAB⁺) *m/z*: (MH⁺) calcd for C₂₀H₂₈N₅O, 354.2294; found, 354.2294. Anal. (C₂₀H₂₇N₅O) C, H, N.

Inhibitor 11b. A mixture of 40 mg of amide **10b** (0.11 mmol) and 20 mg of 2,4,6-trichlorotriazine (0.11 mmol) was reacted in 0.8 mL of DMF. HPFC purification provided **11b** (32 mg, 81%) as a yellow solid: ¹H NMR (DMSO-*d*₆, 400 MHz) δ 0.72 (d, *J* = 6.8 Hz, 3H), 0.82 (t, *J* = 7.1 Hz, 3H), 0.90 (d, *J* = 6.8 Hz, 3H), 1.09–1.34 (m, 4H), 1.68 (s, 3H), 2.12–2.27 (m, 2H), 2.60–2.70 (m, 1H), 6.08 (app t, *J* = 7.6 Hz, 1H), 7.44 (dd, *J* = 1.2, 5.0 Hz, 1H), 7.55 (dd, *J* = 2.9, 5.0 Hz, 1H), 7.87 (s, 1H), 8.16 (dd, *J* = 1.3, 2.9 Hz, 1H), 8.19 (s, 1H); ¹³C NMR (DMSO-*d*₆, 100 MHz) δ 13.8, 17.2, 17.6, 19.8, 21.2, 26.8, 33.0, 34.8, 50.0, 57.3, 117.2, 122.7, 126.5, 127.4, 128.8, 138.5, 151.5, 162.0. HRMS (FAB⁺) *m/z*: (MH⁺) calcd for C₁₈H₂₆N₅O₂S, 360.1858; found, 360.1859. Anal. (C₁₈H₂₅N₅O₂S) C, H, N.

Inhibitor 11c. A mixture of 100 mg of amide **10c** (0.24 mmol) and 44 mg of 2,4,6-trichlorotriazine (0.24 mmol) was reacted in 1.7 mL of DMF. HPLC purification provided **11c** (39 mg, 41%) as a yellow solid: ¹H NMR (400 MHz) δ 0.82–1.11 (m, 6H), 1.15–1.59 (m, 7H), 1.63–1.75 (m, 2H), 1.77–1.88 (m, 2H), 1.89 (s, 3H), 2.20–2.33 (m, 2H), 2.38–2.48 (m, 1H), 5.53 (app t, *J* = 7.4 Hz, 1H), 7.21 (s, 1H), 7.42 (app t, *J* = 7.4 Hz, 2H), 7.50 (t, *J* = 7.4 Hz, 1H), 7.74 (d, *J* = 7.6 Hz, 2H), 7.77 (s, 1H); ¹³C NMR (100 MHz) δ 13.6, 21.3, 21.6, 26.2, 26.3, 27.2, 27.5, 27.6, 34.1, 45.3, 51.3, 58.1, 115.4, 120.9, 126.8, 128.6, 131.7, 134.7, 151.9, 167.5. HRMS (FAB⁺) *m/z*: (MH⁺) calcd for C₂₄H₃₂N₅O, 394.2607; found, 394.2611. Anal. (C₂₁H₃₀N₅O₂S) C, H, N.

Inhibitor 11d. A mixture of 50 mg of amide **10d** (0.12 mmol) and 22 mg of 2,4,6-trichlorotriazine (0.12 mmol) was reacted in 0.8 mL of DMF. HPLC purification provided **11d** (19 mg, 39%) as a yellow solid: ¹H NMR (DMSO-*d*₆, 300 MHz) δ 0.77–1.46 (m, 13H), 1.56–1.90 (m, 7H), 2.13–2.33 (m, 3H), 6.07 (app t, *J* = 10.0 Hz, 1H), 7.44 (dd, *J* = 1.2, 4.8 Hz, 1H), 7.54 (dd, *J* = 2.8, 4.8 Hz, 1H), 7.86 (s, 1H), 8.16 (dd, *J* = 1.2, 2.8 Hz, 1H), 8.18 (s,

1H); ¹³C NMR (100 MHz) δ 13.6, 21.6, 22.2, 26.3, 26.4, 27.3, 27.6, 27.7, 29.7, 34.2, 45.1, 51.2, 58.2, 115.5, 120.3, 126.1, 126.4, 127.9, 138.4, 152.2, 162.2. HRMS (FAB⁺) *m/z*: (MH⁺) calcd for C₂₁H₂₉N₅O₂S, 400.2171; found, 400.2170.

Inhibitor 11e. A mixture of 52 mg of amide **10e** (0.12 mmol) and 22 mg of 2,4,6-trichlorotriazine (0.12 mmol) was reacted in 0.8 mL of DMF. HPFC purification provided **11e** (20 mg, 40%) as a yellow solid: ¹H NMR (400 MHz) δ 0.83 (d, *J* = 6.4 Hz, 3H), 0.86–1.05 (m, 7H), 1.12–1.24 (m, 1H), 1.34–1.50 (m, 4H), 1.55–1.85 (m, 4H), 1.88 (s, 3H), 2.18–2.33 (m, 2H), 2.37–2.46 (m, 1H), 5.52 (app t, *J* = 7.6 Hz, 1H), 7.01 (s, 1H), 7.31 (dd, *J* = 2.8, 5.2 Hz, 1H), 7.38 (dd, *J* = 1.2, 5.2 Hz, 1H), 7.71 (s, 1H), 7.84 (dd, *J* = 1.2, 2.8 Hz, 1H); ¹³C NMR (100 MHz) δ 13.6, 21.6, 22.2, 22.3, 27.2, 27.4, 32.6, 34.2, 34.8, 34.9, 44.7, 51.1, 58.0, 115.5, 120.4, 126.0, 126.4, 127.9, 138.4, 152.1, 162.2. HRMS (FAB⁺) *m/z*: (MH⁺) calcd for C₂₂H₃₂N₅O₂S, 414.2328; found, 414.2335. Anal. (C₂₂H₃₁N₅O₂S) C, H, N.

Synthesis of Chloromethyl Ketone Inhibitor (13). According to literature procedure,²² a 0.2 M solution of 1,2,3-triazole carboxylic acid **12** (90 mg, 0.24 mmol) in 1.2 mL of THF was stirred at –25 °C. To this solution were added 39 μ L of *N*-methylmorpholine (0.34 mmol) and then 41 μ L of isobutyl chloroformate (0.31 mmol). After addition of the chloroformate, a white solid formed. After 1 h, the reaction mixture was filtered and the solid was rinsed with 4 mL of ice-cold THF. The reaction mixture was again stirred at –25 °C until filtration resulted in a clear, colorless solution. Excess diazomethane, prepared from *p*-toluenesulfonylmethylnitrosamide (Diazald), was introduced in situ, according to literature procedure,²³ while the flask was maintained at –25 °C. After the addition of diazomethane, the solution was stirred at –25 °C for 0.5 h and then at room temperature for 0.5 h. In an ice–water bath, a 1:1 solution of concentrated hydrochloric acid and glacial acetic acid was then added dropwise to the solution until the evolution of N₂ was no longer observed. The solution was diluted with EtOAc (15 mL) and transferred to a separatory funnel where it was washed with water (5 mL), satd NaHCO₃ (5 mL), and water (5 mL) until the final water wash was pH neutral. The organic layer was dried (Na₂SO₄), concentrated, and purified by silica gel chromatography (Et₂O/CH₂Cl₂ = 3:97 to 20:80). The ¹H NMR data corresponds to a 1:1 mixture of diastereomers, with about 5% of the methyl ester product observed. ¹H NMR (300 MHz) δ 0.78–1.02 (m, 9H), 1.10–1.23 (m, 1H), 1.23–1.47 (m, 3H), 1.94 (s, 3H), 2.08–2.20 (m, 1H), 2.22–2.36 (m, 1H), 2.90–3.05 (m, 1H), 4.17–4.22 (m, 2H), 5.54 (dd, *J* = 5.1, 10.1 Hz, 1H), 7.29–7.38 (m, 1H), 7.40–7.55 (m, 3H), 7.68–7.76 (m, 1H), 7.77–7.89 (m, 2H). HRMS (FAB⁺) *m/z*: (MH⁺) calcd for C₂₁H₃₀ClN₄O₂, 405.2057; found, 405.2052.

General Assay Procedure. Cathepsins B, K, L, and S were purchased from Calbiochem (San Diego, CA). Cbz-Leu-Arg-AMC, Cbz-Phe-Arg-AMC, 1-*trans*-epoxysuccinyl-Leu-4-guanidinobutylamide (E-64), and 1-*trans*-epoxysuccinyl-Leu-3-methylbutylamide (E-64c) were purchased from Bachem (Torrance, CA). The proteolytic cleavage of *N*-acyl aminocoumarins by cathepsins B, K, L, and S was conducted in Dynatech Microfluor fluorescence 96-well microtiter plates, and readings were taken on a Molecular Devices Spectra Max Gemini XS instrument. The excitation wavelength was 370 nm and the emission wavelength was 455 nm, with a cutoff of 435 nm for AMCA substrates; the excitation wavelength was 355 nm and the emission wavelength was 450 nm for peptidyl-AMC substrates. The assay buffer consisted of a 100 mM solution of pH 6.1 sodium phosphate buffer with 100 mM of sodium chloride, 1 mM of DTT, 1 mM of EDTA, and 0.001% of Tween-20.

Assay Procedure for 1,2,3-Triazole AMCA Substrates. Assays were conducted at 37 °C in duplicate with and without the enzyme. In each well was placed 38 μ L of enzyme solution and 2 μ L of a DMSO substrate solution. Assays were performed at substrate concentrations that were at minimum 10-times less than the *K_m* for that substrate. Relative fluorescent units (RFU) were measured at regular intervals over a period of time (maximum 15 min). A plot of RFU versus time was made for each substrate with and without cathepsin S. The slope of the plotted line gave *V_{max}*/*K_m* of

each substrate for each cathepsin. Using the RFU per μM for AMCA, substrate concentration, and enzyme concentration (determined by E-64 titration for cathepsins B, K, and L or E-64c titration for cathepsin S),²⁴ $k_{\text{cat}}/K_{\text{m}}$ was determined.

To determine the K_{m} and k_{cat} of substrates with cathepsin S, assays were conducted at 37 °C in duplicate with and without the enzyme at six substrate concentrations above and below the K_{m} of each substrate. In each well was placed 190 μL of enzyme solution and 10 μL of a DMSO substrate solution. RFU were measured at regular intervals over a period of time (maximum 15 min). A plot of RFU/s versus substrate concentration, analyzed using Kaleida-Graph, was used to determine K_{m} and V_{max} . Using the RFU per μM for AMCA and the cathepsin S concentration (determined by E-64c titration),²⁴ k_{cat} was determined.

Assay Procedure for Nitrile Inhibitors. The dissociation constants (K_{i}) were calculated by the method of Dixon.²⁵ Cathepsin B concentration in the assays was 2 nM; cathepsin K concentration in the assays was 10 nM; cathepsin L concentration in the assays was 0.03 nM; and cathepsin S concentration in the assays was 0.6 nM. Two concentrations of Cbz-Phe-Arg-AMC (5 μM and 2.5 μM for cathepsins B and K, 0.6 μM and 0.3 μM for cathepsin L) or Cbz-Leu-Arg-AMC (5 μM and 2.5 μM for cathepsin S) were used. Assays were conducted in duplicate with and without inhibitor at five inhibitor concentrations to provide 10–90% enzyme inhibition. In each well was placed 180 μL of enzyme solution and 10 μL of a DMSO inhibitor solution. The resulting solutions were incubated for 5 min at 37 °C, and then 10 μL of the peptidyl-AMC substrate was added and generation of AMC was monitored over 5 min.

Crystallization and Data Collection. Cathepsin S was expressed in the baculovirus system and its complex with inhibitor **13**, produced by adding **13** to the protein in a 2:1 molar ratio prior to concentration of the protein to 15 mg/mL. A coarse screen of 480 crystallization conditions was set up in low profile 96-well Greiner plates at 4 °C in a sitting drop format containing 250 nL of protein combined with an equal volume of crystallization solution. Crystals appeared after 1–2 weeks in two distinct crystal forms. Data were collected at beamline 5.0.3 of the Advanced Light Source (ALS) in Berkeley, CA. The two crystal forms belong to space groups $P4_122$ and $P6_522$ and diffracted to 1.5 and 1.9 Å, respectively (data statistics are presented in Table 2). The tetragonal crystal form was isomorphous with a previously determined crystal form,^{5d} while that of the hexagonal crystal form was solved by molecule replacement using this model as a search probe with MOLREP.²⁶ Both structures were then iteratively refined until convergence with *coot*²⁷ and *refmac5*,²⁸ all other crystallographic manipulations were carried out with the CCP4 program package.²⁹ Both structures exhibited excellent geometry, with no residues in disallowed regions of the Ramachandran plot. The two crystals contained two and three molecules per asymmetric unit, providing five separate structures of compound binding that were essentially identical. The structures were deposited with PDB code 2H7J and 2HXZ.

Acknowledgment. J.A.E., W.J.L.W., and A.W.P. gratefully acknowledge the NIH (GM54051) for support of this work. A.W.P. greatly appreciates an American Chemical Society Medicinal Chemistry Graduate Student Fellowship sponsored by Bristol Myers Squibb. The authors would also like to thank Andreas Kreuzsch, Mike Didonato, and Christian Lee for help with data collection and Peter Schultz for continued support and encouragement. The work in this paper is based on experiments conducted at beamline 5.0.3 of the advanced light source (ALS). The ALS is supported by the Director, Office of Science, Office of Basic Energy Sciences, Material Sciences Division of the U.S. Department of Energy under Contract No. DE-AC03-76SF00098 at Lawrence Berkeley National Laboratory. We would like to thank all of the staff at these beamlines for their continued support.

Supporting Information Available: Purity data of compounds **8** and **11**. Data for the X-ray crystal structures have been deposited

in the Protein Data Bank; PDB ID: 2H7J and 2HXZ. This material is available free of charge via the Internet at <http://pubs.acs.org>.

References

- (1) Wood, W. J. L.; Patterson, A. W.; Tsuruoka, H.; Jain, R. K.; Ellman, J. A. Substrate Activity Screening: A fragment-based method for the rapid identification of nonpeptidic protease inhibitors. *J. Am. Chem. Soc.* **2005**, *127*, 15521–15527.
- (2) Salisbury, C. M.; Ellman, J. A. Rapid identification of potent nonpeptidic serine protease inhibitors. *ChemBioChem* **2006**, *7*, 1034–1037.
- (3) For recent reviews on fragment-based methods, see: (a) Erlanson, D. A.; McDowell, R. S.; O'Brien, T. Fragment-based drug discovery. *J. Med. Chem.* **2004**, *47*, 3463–3482. (b) Carr, R. A. E.; Congreve, M.; Murray, C. W.; Rees, D. C. Fragment-based lead discovery: Leads by design. *Drug Discovery Today* **2005**, *10*, 987–992. (c) Hartshorn, M. J.; Murray, C. W.; Cleasby, A.; Frederickson, M.; Tickle, I. J.; Jhoti, H. Fragment-based lead discovery using X-ray crystallography. *J. Med. Chem.* **2005**, *48*, 403–413.
- (4) (a) McGovern, S. L.; Caselli, E.; Grigorieff, N.; Shoichet, B. K. A common mechanism underlying promiscuous inhibitors from virtual and high-throughput screening. *J. Med. Chem.* **2002**, *45*, 1712–1722. (b) McGovern, S. L.; Helfand, B. T.; Feng, B.; Shoichet, B. K. A specific mechanism of nonspecific inhibition. *J. Med. Chem.* **2003**, *46*, 4265–4272. (c) McGovern, S. L.; Shoichet, B. K. Kinase inhibitors: Not just for kinases anymore. *J. Med. Chem.* **2003**, *46*, 1478–1483.
- (5) (a) Leroy, V.; Thurairatnam, S. Cathepsin S inhibitors. *Expert Opin. Ther. Pat.* **2004**, *14*, 301–311. (b) Yasuda, Y.; Kaleta, J.; Broemme, D. The role of cathepsins in osteoporosis and arthritis: Rationale for the design of new therapeutics. *Adv. Drug Delivery Rev.* **2005**, *57*, 973–993. (c) Leung-Toung, R.; Zhao, Y.; Li, W.; Tam, T. F.; Karimian, K.; Spino, M. Thiol proteases: inhibitors and potential therapeutic targets. *Curr. Med. Chem.* **2006**, *13*, 547–581. (d) Tully, D. C.; Liu, H.; Alper, P. B.; Chatterjee, A. K.; Epple, R.; Roberts, M. J.; Williams, J. A.; Nguyen, K. T.; Woodmansee, D.; Tumanut, C.; Li, J.; Spraggon, G.; Chang, J.; Tuntland, T.; Harris, J. L.; Karanewsky, D. S. Synthesis and evaluation of arylaminoethyl amides as noncovalent inhibitors of cathepsin S. Part 3: Heterocyclic P3. *Bioorg. Med. Chem. Lett.* **2006**, *16*, 1975–1980.
- (6) Gocheva, V.; Zeng, W.; Ke, D.; Klimstra, D.; Reinheckel, T.; Peters, C.; Hanahan, D.; Joyce, J. A. Distinct roles for cysteine cathepsin genes in multistage tumorigenesis. *Genes Dev.* **2006**, *20*, 543–556.
- (7) (a) Rawlings, N. D.; Barrett, A. I. Families of cysteine proteases. *Methods Enzymol.* **1994**, *244*, 461–486. (b) Cygler, M.; Mort, J. S. Proregion structure of members of the papain superfamily: Mode of inhibition of enzymic activity. *Biochimie* **1997**, *79*, 645–652.
- (8) Villhauer, E. B.; Brinkman, J. A.; Naderi, G. B.; Burkey, B. F.; Dunning, B. E.; Prasad, K.; Mangold, B. L.; Russell, M. E.; Hughes, T. E. 1-[[3-(3-Hydroxy-1-adamantyl)amino]acetyl]-2-cyano-(S)-pyrrolidine: A potent, selective, and orally bioavailable dipeptidyl peptidase IV inhibitor with antihyperglycemic properties. *J. Med. Chem.* **2003**, *46*, 2774–2789.
- (9) Cogan, D. A.; Liu, G.; Ellman, J. A. Asymmetric synthesis of chiral amines by highly diastereoselective 1,2-additions of organometallic reagents to *N-tert*-butanesulfinyl imines. *Tetrahedron* **1999**, *55*, 8883–8904.
- (10) Patterson, A. W.; Ellman, J. A. Asymmetric synthesis of α,α -dibranched propargylamines by acetylide additions to *N-tert*-butanesulfinyl ketimines. *J. Org. Chem.* **2006**, *71*, 7110–7112.
- (11) Tornøe, C. W.; Christensen, C.; Meldal, M. Peptidotriazoles on solid phase: [1,2,3]-Triazoles by regioselective copper(I)-catalyzed 1,3-dipolar cycloadditions of terminal alkynes to azides. *J. Org. Chem.* **2002**, *67*, 3057–3064.
- (12) PDB ID: 2H7J
- (13) PDB ID: 2HXZ
- (14) McGrath, M. E. The lysosomal lysine proteases. *Annu. Rev. Biophys. Biomol. Struct.* **1999**, *28*, 181–204.
- (15) (a) Russell, R. B.; Barton, G. J. Multiple protein sequence alignment from tertiary structure comparison. *Proteins: Struct., Funct., Genet.* **1992**, *14*, 309–323. (b) Barton, G. J. ALSCRIPT: A tool to format multiple sequence alignments. *Protein Eng.* **1993**, *6*, 37–40.
- (16) (a) Bromme, D.; Klaus, J. L.; Okamoto, K.; Rasnick, D.; Palmer, J. T. Peptidyl vinyl sulfones: A new class of potent and selective cysteine protease inhibitors. S2P2 specificity of human cathepsin O2 in comparison with cathepsins S and L. *Biochem. J.* **1996**, *315*, 85–89. (b) Marquis, R. W.; James, I.; Zeng, J.; Trout, R. E. L.; Thompson, S.; Rahman, A.; Yamashita, D. S.; Xie, R.; Ru, Y.; Gress, C. J.; Blake, S.; Lark, M. A.; Hwang, S.-M.; Tomaszek, T.; Offen, P.; Head, M. S.; Cummings, M. D.; Veber, D. F. Azepanone-based

- inhibitors of human cathepsin L. *J. Med. Chem.* **2005**, *48*, 6870–6878. (c) Loser, R.; Schilling, K.; Dimmig, E.; Gutschow, M. Interaction of papain-like cysteine proteases with dipeptide-derived nitriles. *J. Med. Chem.* **2005**, *48*, 7688–7707.
- (17) Phillips, M. A.; Kaplan, A. P.; Rutter, W. J.; Bartlett, P. A. Transition-state characterization: A new approach combining inhibitor analogues and variation in enzyme structure. *Biochemistry* **1992**, *31*, 959–963.
- (18) Mader, M. M.; Bartlett, P. A. Binding energy and catalysis: The implications for transition-state analogues and catalytic antibodies. *Chem. Rev.* **1997**, *97*, 1281–1301.
- (19) Maly, D. J.; Leonetti, F.; Backes, B. J.; Dauber, D. S.; Harris, J. L.; Craik, C. S.; Ellman, J. A. Expedient solid-phase synthesis of fluorogenic protease substrates using the 7-amino-4-carbamoylmethylcoumarin (ACC) fluorophore. *J. Org. Chem.* **2002**, *67*, 910–915.
- (20) Lundquist, J. T., IV; Pelletier, J. C. Improved solid-phase peptide synthesis method utilizing α -azide-protected amino acids. *Org. Lett.* **2001**, *3*, 781–783.
- (21) Purity was determined to be >95%, analyzed by HPLC, as described for substrates **8**.
- (22) Krantz, A.; Copp, L. J.; Coles, P. J.; Smith, R. A.; Heard, S. B. Peptidyl (acyloxy)methyl ketones and the quiescent affinity label concept: the departing group as a variable structural element in the design of inactivators of cysteine proteinases. *Biochemistry* **1991**, *30*, 4678–4687.
- (23) Lombardi, P. A rapid, safe, and convenient procedure for the preparation and use of diazomethane. *Chem. Ind. (London)* **1990**, 708.
- (24) Barrett, A. J.; Kembhavi, A. A.; Brown, M. A.; Kirschke, H.; Knight, C. G.; Tamai, M.; Hanada, K. L-*trans*-Epoxysuccinyl-leucylamido-(4-guanidino)butane (E-64) and its analogues as inhibitors of cysteine proteinases including cathepsins B, H, and L. *Biochem. J.* **1982**, *201*, 189–198.
- (25) Dixon, M. Determination of enzyme–inhibitor constants. *Biochem. J.* **1953**, *55*, 170–171.
- (26) Vagin, A.; Teplyakov, A. An approach to multi-copy search in molecular replacement. *Acta Crystallogr., Sect. D* **2000**, *56*, 1622–1624.
- (27) Emsley, P.; Cowtan, K. Coot: Model-building tools for molecular graphics. *Acta Crystallogr., Sect. D* **2004**, *60*, 2126–2132.
- (28) Murshudov, G. N.; Vagin, A. A.; Dodson, E. J. Refinement of macromolecular structures by the maximum-likelihood method. *Acta Crystallogr., Sect. D* **1997**, *53*, 240–255.
- (29) Collaborative; Computing; Project; Number 4 The CCP4 suite: Programs for protein crystallography, Version 3.1. *Acta Crystallogr., Sect. D* **1994**, *50*, 760–763.

JM060701Sz